

Multi-Graph Fusion Networks for Urban Region Embedding

Shangbin Wu^{*1} Xu Yan^{*1}, Xiaoliang Fan^{†1} Shirui Pan² Shichao Zhu³ Chuanpan Zheng¹ Ming Cheng¹ Cheng Wang¹

¹Xiamen University

²Monash University

³University of Chinese Academy of Sciences

{shangbin, yanxu97, zhengchuanpan}@stu.xmu.edu.cn, {fanxiaoliang, chm99, cwang}@xmu.edu.cn
shirui.pan@monash.edu, zhushichao@ie.ac.cn

Abstract

Learning the embeddings for urban regions from human mobility data can reveal the functionality of regions, and then enables the correlated but distinct tasks such as crime prediction. Human mobility data contains rich but abundant information, which yields to the comprehensive region embeddings for cross domain tasks. In this paper, we propose multi-graph fusion networks (MGFN) to enable the cross domain prediction tasks. First, we integrate the graphs with spatio-temporal similarity as mobility patterns through a *mobility graph fusion module*. Then, in the *mobility pattern joint learning module*, we design the multi-level cross-attention mechanism to learn the comprehensive embeddings from multiple mobility patterns based on intra-pattern and inter-pattern messages. Finally, we conduct extensive experiments on real-world urban datasets. Experimental results demonstrate that the proposed MGFN outperforms the state-of-the-art methods by up to 12.35% improvement.

1 Introduction

Revealing urban region embedding aims to learn quantitative representations of regions from multi-sourced data, such as Point-of-Interests (POI), check-in, and human mobility [Wang and Li, 2017]. Human mobility data reflects the human interactions and cooperation, and thus can be used to conduct distinct tasks such as epidemic [Wu *et al.*, 2021], economics [Xu *et al.*, 2020], crime [Xia *et al.*, 2021] prediction, etc.

The cross-domain downstream tasks such as crime prediction and check-in prediction, are used to verify the effectiveness of region embeddings. Existing studies [Du *et al.*, 2019; Wang and Li, 2017; Yao *et al.*, 2018] taking all detailed time-series mobility records as input, could merely learn a specific representation (e.g., change of traffic flows), rather than generalized urban region embeddings.

^{*}These authors contributed equally to this work

[†]Corresponding author: fanxiaoliang@xmu.edu.cn

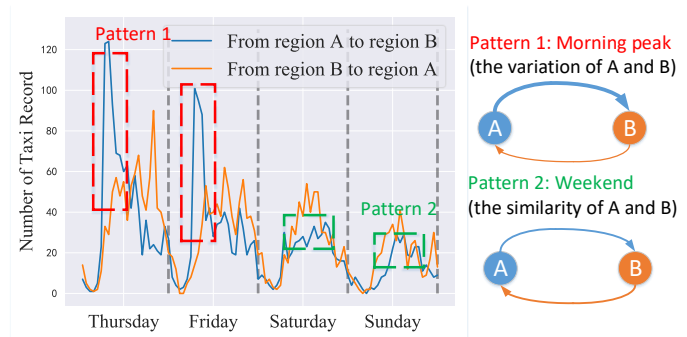


Figure 1: A motivating example. The complexity of mobility patterns depends on both urban periodicity and regional functionality distribution. For two regions (A is a residential area, and B is a office area), there could be two distinct patterns (i.e., variation, similarity).

Human mobility data contains both abundant information and complex patterns [Hou and Li, 2016], which yields to the comprehensive region embeddings for cross domain tasks. For example, Figure 1 (left) shows two repeated patterns, which can be integrated as Pattern 1 (morning peak) and Pattern 2 (weekend) respectively. Figure 1 (right) shows the complexity of mobility patterns that there are two distinct patterns (i.e., variation and similarity). Measuring a generalized region embeddings from abundant human mobility data is challenging:

Challenge 1: How to process the fine-grained mobility data to learn a generalized embedding? In our considered scenario, learning from abundant human mobility data may only attain the change of mobility flows, rather than a generalized embedding.

Solution 1: Mobility graph fusion. To attain an effective and generalized embedding from abundant human mobility data, we first approach regions as interactive and interdependent nodes by constructing the human mobility data as mobility multi-graph. Then, we aggregate mobility graphs as selected mobility patterns according to the spatio-temporal distance between any two mobility graphs.

Challenge 2: How to jointly learn from mobility patterns? Training a separate pattern mining model on each of them may not capture comprehensive representation of regional characteristics.

Solution 2: Mobility Pattern Joint Learning. The constructed mobility graphs possess regularized characteristics, which are fully connected, directed, and weighted with multiple edges (i.e., multi-graph). Different from previous graph representation models [Zhang *et al.*, 2020], we take advantage of above characteristics by designing two modules: (1) Intra-pattern message passing, which utilizes structural information inside each graph to learn a local embedding; and (2) Inter-pattern message cross attention, which conducts attention mechanism among different graphs to jointly learn comprehensive region embeddings.

The major contributions of this paper are:

- We study the urban region representation problem on fine-grained human mobility data, and propose a mobility graph fusion module with spatio-temporal dependencies where redundant graphs are integrated as patterns.
- We propose a mobility pattern joint learning module, which learns the region embedding from intra-pattern message and inter-pattern message simultaneously in a new manner, with the hope that the cross-graph information can mutually enhance each other.
- Extensive experimental results show that our mobility graph fusion method can effectively uncover the complex mobility patterns. And our method outperforms state-of-the-art baselines up to 12.35% in crime and check-in prediction tasks in terms of various metrics.

2 Problem Statement

We provide necessary preliminary concepts in this work, and formalize the problem of urban region embedding.

Definition 1 (Mobility Graph). *The mobility graph at the time step t is defined as a directed and weighted graph $G_t = (V, E_t)$, where V denotes the node set with node $v_i \in V$ representing region v_i , and E_t denotes the edge set with edge $e_{ij}^t = (v_i, v_j, \omega_{ij}^t) \in E$ representing the number of people ω_{ij}^t move from urban region v_i to v_j at time t .*

Definition 2 (Mobility Multi-graph). *It is defined as a directed and weighted multi-graph $G = \cup_{t=0}^{T-1} \{G_t = (V, E_t)\}$, where G_t is a mobility graph at time t , and V denotes the node set that corresponds to regions, and E_t denotes the edge set that corresponds to mobility condition at time t .*

Definition 3 (Mobility Pattern). *The mobility patterns $\mathcal{G} = \{\mathcal{G}_0, \mathcal{G}_1, \dots, \mathcal{G}_{N-1}\}$ are the result of fusing similar mobility multi-graph. A pattern \mathcal{G}_k is also a directed and weighted graph with the same node set V as mobility multi-graph.*

Definition 4 (Urban Region Embedding). *Given the urban human mobility multi-graph G , the goal of urban region embedding is to learn a mapping function $\phi : v_i \rightarrow \mathbb{R}^d$ to generate distributed and low dimensional embedding $\hat{H} \in \mathbb{R}^{|V| \times d}$ of each urban region $v_i \in V$, where d represents the dimension of urban region embeddings.*

3 Methodology

In this section, we first introduce the mobility graph fusion module, in which we propose a novel Mobility Graph

Distance (MGD) to measure the similarity between different mobility graphs. Then, we present an effective mobility pattern joint learning module, which contains intra-pattern message passing and inter-pattern message cross attention to capture comprehensive regional characterise by mobility patterns. Figure 2 shows the overall architecture of our proposed multi-graph fusion network.

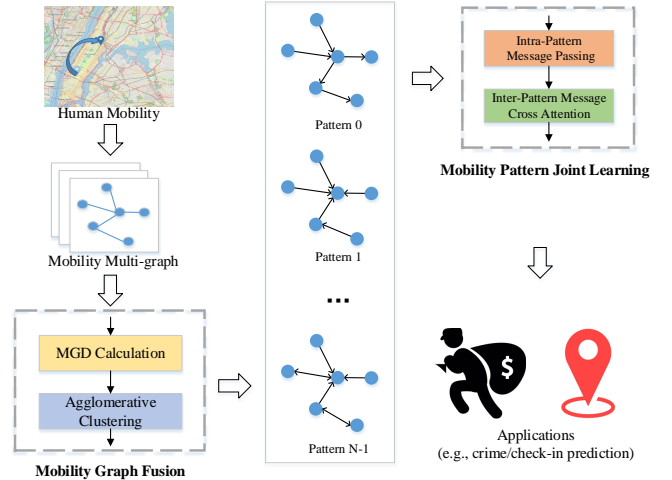


Figure 2: MGFN Framework. The architecture transforms human mobility patterns into representation abilities for downstream tasks (e.g., crime, check-in prediction). Our framework consists of two modules: 1) Mobility Graph Fusion module where time-series multi-graph are fused by a Mobility Graph Distance (MGD) measurement method; and 2) Mobility Pattern Joint Learning module (detailed in Figure 3) which learns the region embedding by both intra-pattern message and inter-pattern message.

3.1 Mobility Graph Fusion

Human mobility reveals the functions and properties of urban regions [Wang and Li, 2017]. Our intuition is that mobility patterns are able to describe the urban region functionality thus in favour of learning the generalized representation of urban regions. For example, we can estimate whether a region is work area or residential area according to the mobility direction of people during the morning peak hours (i.e., 7-9 a.m.). Therefore, based on the aim of extracting mobility patterns with the urban region functionality, rather than how human mobility changes, we model the problem as time-series human mobility multi-graph fusion to generate the mobility patterns. In detail, we define mobility graph distance (MGD) to calculate the distance between mobility graphs, and then aggregate human mobility data according to their similarity.

Spatial Structure Distance on Mobility Graph

Data with similar mean and variance may have higher similarity. Specifically, for mobility graphs, we assume that the weights on its edges are sampled from a Gaussian distribution, and calculate its mean and variance:

$$\mu_G = \frac{1}{|E|} \sum_{e \in E} e, \quad \sigma_G^2 = \frac{1}{|E|} \sum_{e \in E} (e - \mu_G)^2. \quad (1)$$

Then, the mean distance and variance distance between the mobility graph G_a and G_b are expressed as:

$$D_{mean}(G_a, G_b) = \|\mu_{G_a} - \mu_{G_b}\|, \quad (2)$$

$$D_{var}(G_a, G_b) = \|\sigma_{G_a}^2 - \sigma_{G_b}^2\|. \quad (3)$$

It is not sufficient to only compare the mean and variance. For example, The mean and variance of the morning and evening rush hours are similar, but their destinations are different (working and residential areas, respectively). So we also pay attention to flow imbalance of two regions, and highlight the high traffic flow. Specifically, we first propose the unidirectional flow distance defined as follows:

$$D_{unif}(G_a, G_b) = \|UniF(G_a) - UniF(G_b)\| \quad (4)$$

where $UniF(G_t) = \sum_{v_i \in V} \sum_{v_j \in V} \|\omega_{ij}^t - \omega_{ji}^t\|$ is the unidirectional flow index of the graph.

Then, we label the edges with high weights in the graph, G_t is encoded as a spatial structure label matrix \mathcal{E}^t , in which each element \mathcal{E}_{ij}^t represents whether the weight ω_{ij}^t of edge e_{ij}^t in G_t is large enough. It greatly simplifies the mobility graph and highlights the high-weight edges, given as follows.

$$\mathcal{E}_{ij}^t = \begin{cases} 1 & \omega_{ij}^t > \mu_{ij} \\ 0 & \omega_{ij}^t \leq \mu_{ij} \end{cases}, \quad (5)$$

where $\mu_{ij} = \frac{1}{T} \sum_{t=1}^T \omega_{ij}^t$ represents the mean value of edge weight between node v_i and v_j over the time series.

Afterwards, we define the spatial structure encoding distance between mobility graphs G_a and G_b :

$$D_{ss}(G_a, G_b) = \|\mathcal{E}_a \oplus \mathcal{E}_b\|_1, \quad (6)$$

where \oplus is the xor operation, \mathcal{E}_a and \mathcal{E}_b denote the spatial structure label matrix of G_a and G_b respectively.

Temporal Aggregation with Mobility Graph Distance

After considering the statistical distance and spatial structure distance between mobility graphs, we take temporal similarity into account. We define mobility graph distance as the sum of above distance weighted by the temporal similarity with a non-linearity, given as follows:

$$MGD(G_a, G_b) = Z(\Delta t) \sum c_i M(D_i), \quad (7)$$

where c_i is the weight of i -th distance, and D_i could be $D_{mean}, D_{var}, D_{unif}, D_{ss}$, $M(\cdot)$ denotes the normalization function such as MinMaxScaler, $Z(\cdot)$ is an activation function. Δt denotes the time interval between G_a and G_b . Our intuition is that two mobility graphs with close temporal distance are similar.

Finally, we calculate the distance between mobility graphs through MGD, and use the clustering method (i.e., agglomerative cluster) to aggregate mobility graphs with different patterns thus to generate mobility patterns \mathcal{G} .

3.2 Mobility Pattern Joint Learning

The above Mobility Graph Fusion (MGF) module extracts important mobility patterns by aggregating plentiful redundant mobility data based on the proposed MGD metric. In order to learn the underlying information of urban regions from

mobility patterns, we present a mobility pattern joint learning module as shown in Figure 3. The proposed framework mainly consists of two parts: intra-pattern message passing (IPMP) and inter-pattern message cross attention (IPMCA). In the first part, the region hidden representations are updated by intra-pattern message propagating and aggregating in each mobility pattern thus extracting the spatial correlation between regions. In the second part, the cross-attention mechanism is used to integrate the inter-pattern message between the different mobility patterns for each region. Comprehensive embeddings output by two parts with residual connections [He *et al.*, 2016] are integrated by a fully connected layer to generate the final region embeddings.

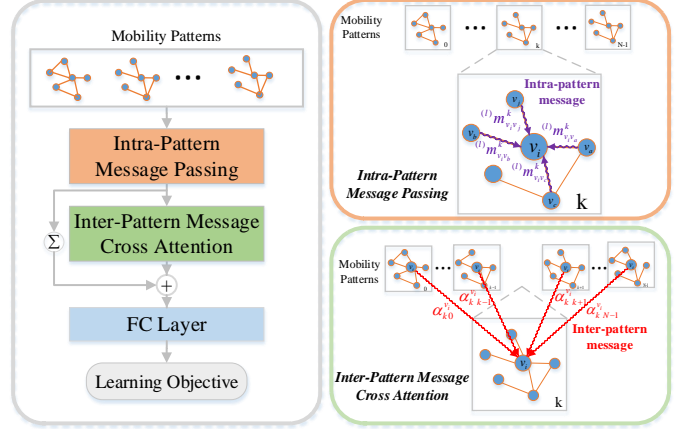


Figure 3: The architecture of mobility pattern joint learning module (left) consists: (1) intra-pattern message passing (upper right), (2) inter-pattern message cross attention (down right) and (3) a fully connected layer. The former propagates and aggregates intra-pattern message to generate region hidden representation in N patterns. The latter obtains a fused region embeddings by cross-attention mechanism using inter-pattern message.

Intra-Pattern Message Passing

The property of an urban region is affected by other regions with different impacts due to the spatial correlations. We assume that such impact is highly correlated to the human mobility condition including in-flow and out-flow for a region. To capture the spatial correlations, inspired by [Gilmer *et al.*, 2017], we design a intra-pattern message passing layer to propagate the inner flow messages between different regions in each mobility pattern.

This part takes mobility patterns \mathcal{G} as input. We initialize the 0^{th} -layer hidden representations of regions v_i in mobility pattern \mathcal{G}_k as input region features $x_{v_i}^k$, i.e.: ${}^{(0)}h_{v_i}^k = x_{v_i}^k$. Considering the mobility flow from region v_j to region v_i , inspired by [Veličković *et al.*, 2017], we compute the message sent along the mobility flow edge $v_j \rightarrow v_i$ by self-attention mechanism. The message function is defined as follows:

$$m_{v_i v_j}^k = \frac{\exp\left(\left\langle W_{q^p} h_{v_i}^k, W_{k^p} h_{v_j}^k \right\rangle / \sqrt{d}\right)}{\sum_{v_b \in N(v_i)} \exp\left(\left\langle W_{q^p} h_{v_i}^k, W_{k^p} h_{v_b}^k \right\rangle / \sqrt{d}\right)}, \quad (8)$$

where $\langle \cdot, \cdot \rangle$ is inner product, W_{q^p} and W_{k^p} are two trainable projection matrices, d is the dimension node hidden representation and $N(v_i)$ is the neighbor region set of v_i . Here, the message from region v_j to v_i is also the attention score.

Afterwards, region v_i aggregates the messages sent by its neighbor regions $N(v_i)$, and updates its hidden representation by a weighed sum from $N(v_i)$, given as follows.

$${}^{(l)}h_{v_i}^k = \sum_{v_j \in N(v_i)} m_{v_i v_j}^k {}^{(l)}W_{v^p}^{(l-1)} h_{v_j}^k, \quad (9)$$

where ${}^{(l)}W_{v^p}$ is a learnable projection matrix in l^{th} layer. Here, as the mobility pattern is a directed complete graph, the neighbors of each region are all the regions, i.e., $N(v_i) = V, v_i \in V$.

To stabilize the learning process and learn information at different conceptual levels, we extend the self-attention mechanism to be multi-head ones [Vaswani *et al.*, 2017]. Specifically, we concatenate F parallel attention message functions with different learnable projections:

$${}^{(l)}h_{v_i}^k = \parallel_{f=1}^F \left\{ \sum_{v_j \in V} {}^{(f)}m_{v_i v_j}^k {}^{(f,l)}W_{v^p}^{(l-1)} h_{v_j}^k \right\}, \quad (10)$$

where \parallel represents concatenation operation, and ${}^{(f)}f_{v_i v_j}^k$ represents the attention score calculated by the message function in the f^{th} head attention.

Taking the importance of mobility directions and the difference between in-flow and out-flow mobility for a region into account, we divide each mobility pattern \mathcal{G}_k into two parts: source mobility pattern \mathcal{G}_k^s and target mobility pattern \mathcal{G}_k^t . Here, we regard the out-flow and in-flow mobility as node features of source intra-pattern X_k^s and target intra-pattern X_k^t , and apply intra-message passing layer in these two type of patterns, respectively, where $X_k^s = X_k^{t\top}$. To fuse these two region representations, we project the concatenation of them to generate hidden representation of v_i :

$${}^{(l)}h_{v_i}^k = f({}^{(l)}h_{v_i}^k \parallel {}^{(l)}h_{v_i}^k) \quad (11)$$

where $f(\cdot)$ represents a linear projection. The region hidden representations extracting spatial dependency of N mobility patterns $h_{v_i} = \{h_{v_i}^0, h_{v_i}^1, \dots, h_{v_i}^{N-1}\}$ are generated by stacking L intra-pattern message passing layers.

Inter-Pattern Message Cross Attention

Intra-pattern message passing provides a robust mechanism for capturing the spatial correlations between urban regions in each mobility pattern. For learning the cross interactions between different mobility patterns for a region, we allow region to interact across mobility patterns via a self-attention mechanism [Vaswani *et al.*, 2017].

Considering the region v_i in mobility pattern \mathcal{G}_a and \mathcal{G}_b , let the node features in mobility pattern \mathcal{G}_a and \mathcal{G}_b are $h_{v_i}^a$ and $h_{v_i}^b$. Then, for every such pair, we compute the correlation between \mathcal{G}_a and \mathcal{G}_b using self-attention as follows:

$$\alpha_{ab}^{v_i} = \frac{\exp(\langle W_{q^c} h_{v_i}^a, W_{k^c} h_{v_i}^b \rangle / \sqrt{d})}{\sum_{k=0}^{N-1} \exp(\langle W_{q^c} h_{v_i}^a, W_{k^c} h_{v_i}^k \rangle / \sqrt{d})}, \quad (12)$$

where W_{q^c} and W_{k^c} are two trainable projection matrices, and $\alpha_{ab}^{v_i}$ is the attention score revealing how \mathcal{G}_a attends to the

features of region v_i of \mathcal{G}_b . Afterwards, we compute an inter-pattern message for the region v_i of mobility pattern \mathcal{G}_a by a weighed sum (i.e., attention), where the multi-head attention is applied again:

$$h_{v_i}^a = \parallel_{f=1}^F \left\{ \sum_{k=0}^{N-1} \alpha_{ak}^{v_i} W_{v^c} h_{v_i}^k \right\}, \quad (13)$$

where W_{v^c} is a learnable projection matrix.

Finally, the fused region embedding of v_i is updated as the result of aggregating the inter-pattern message with mean aggregator as follows:

$$\bar{h}_{v_i} = \frac{1}{N} \sum_{k=0}^{N-1} h_{v_i}^k \quad (14)$$

Objective Function

With the residual connection of intra-pattern message passing, we use a fully connected layer as an output layer to obtain the final region embeddings \hat{h}_{v_i} :

$$\hat{h}_{v_i} = f\left(\frac{1}{N} \sum_{k=0}^{N-1} h_{v_i}^k + \bar{h}_{v_i}\right), \quad (15)$$

Following [Wang and Li, 2017; Zhang *et al.*, 2020], we use region embedding to estimate the distribution of mobility flow, and learn the embedding by minimizing the difference between the true distribution and the estimated distribution. Given the source region v_i , we calculate the transition probability of destination region v_j as follow:

$$p_{\omega}(v_j|v_i) = \frac{\omega_{ij}}{\sum_{v_{j^*} \in N(v_i)} \omega_{ij^*}}, \quad (16)$$

where ω_{ij} refers to the mobility flow from v_i to v_j , and $N(v_i)$ refers to the neighbors of v_i . Then, given the region embedding $\hat{h}_{v_i}, \hat{h}_{v_j}$ for region v_i, v_j , we estimate the transition probability:

$$\hat{p}_{\omega}(v_j|v_i) = \frac{\exp(\hat{h}_{v_i}^{\top} \hat{h}_{v_j})}{\sum_{v_{j^*} \in N(v_i)} \exp(\hat{h}_{v_i}^{\top} \hat{h}_{v_{j^*}})}, \quad (17)$$

Finally, the objective function can be expressed as:

$$\mathcal{L} = \sum_{i,j} -p_{\omega}(v_j|v_i) \log \hat{p}_{\omega}(v_j|v_i). \quad (18)$$

4 Evaluation

This section aims to answer the following research questions:

RQ1 How is the performance of our MGFN as compared to various state-of-the-art methods?

RQ2 How do different components (e.g., mobility graph fusion, mobility pattern joint learning) affect the results?

RQ3 Can the proposed mobility graph fusion module really discover mobility patterns? What are its advantages compared with other methods?

RQ4 Why did other models perform worse than ours? Is it true that the other methods learned how traffic flow changes? (as we assume in Section 1)

4.1 Experiment Settings

Data Description We evaluate the performance of our method on New York City (NYC) datasets from NYC open data website¹. We follow the settings in [Zhang *et al.*, 2020] and apply taxi trip data as human mobility data and take the crime count, check-in count, land usage type as prediction tasks, respectively.

Baselines We compare MGFN with the following baseline methods: (1) **node2vec** [Grover and Leskovec, 2016] uses biased random walks to learn node latent representations by skip-gram models; (2) **LINE** [Tang *et al.*, 2015] optimizes the objective function that preserves both the local and global network structures. (3) **HDGE** [Wang and Li, 2017] jointly embeds a spatial graph and a flow graph with temporal dynamics. (4) **ZE-Mob** [Yao *et al.*, 2018] captures massive human mobility patterns, and models spatio-temporal co-occurrence of zones in the embedding learning; (5) **MV-PN** [Fu *et al.*, 2019] learns region embeddings with multi-view PoI network within the region; (6) **MVURE** [Zhang *et al.*, 2020] enable cross-view information sharing and weighted multi-view fusion with human mobility and inherent region attributes data (e.g. POI, check-in).

Parameter Settings Following [Zhang *et al.*, 2020], the dimension region embeddings d is set as 96. In the Mobility graph fusion module, the weight in MGD calculation c_i is set as 1, and the number of mobility patterns N is set as 7. In the mobility pattern joint learning module, the number of layers L in is set as 1.

4.2 Performance Comparison (RQ1)

For regression tasks (i.e., crime, check-in), we apply the Lasso regression [Tibshirani, 1996] with metrics of Mean Absolute Error (MAE), Root Mean Square Error (RMSE) and coefficient of determination (R^2). For the clustering task (i.e., land usage classification), we use K-means to cluster region embeddings with Normalized Mutual Information (NMI) and Adjusted Rand Index (ARI) with settings in [Yao *et al.*, 2018].

Table 1 shows the results of crime prediction, land usage classification and check-in count prediction. We observe that: (1) deep learning approaches outperform traditional graph embedding methods, and graph modeling methods (i.e., MGFN, MVURE) generally perform better than HDGE, ZE-Mob and MV-PN, indicating the spatial dependency between regions is a necessity for urban region embedding; and (2) although MGFN utilizes less data (i.e., human mobility only) than the second best model MVURE, our algorithm achieves state-of-the-art prediction performances, and achieves up to 12.35% improvement in terms of RMSE in crime prediction.

4.3 Model Ablation Study (RQ2)

To further investigate the effect of each component in our model, we compare MGFN with its three variants by removing multi graph fusion module, intra-pattern message passing and inter-pattern message cross attention in mobility pattern joint learning module from our method separately, which are

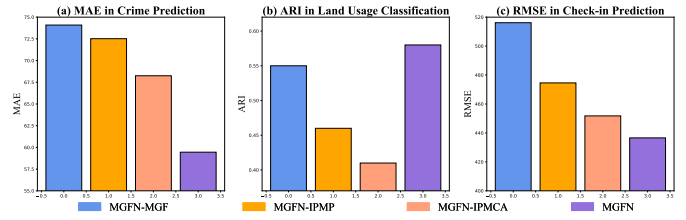


Figure 4: Ablation studies for three tasks on NYC dataset. (a) MAE in Crime Prediction. (b) ARI in Land Usage Classification. (c) RMSE in Check-in Prediction. The results demonstrate the effectiveness of each component.

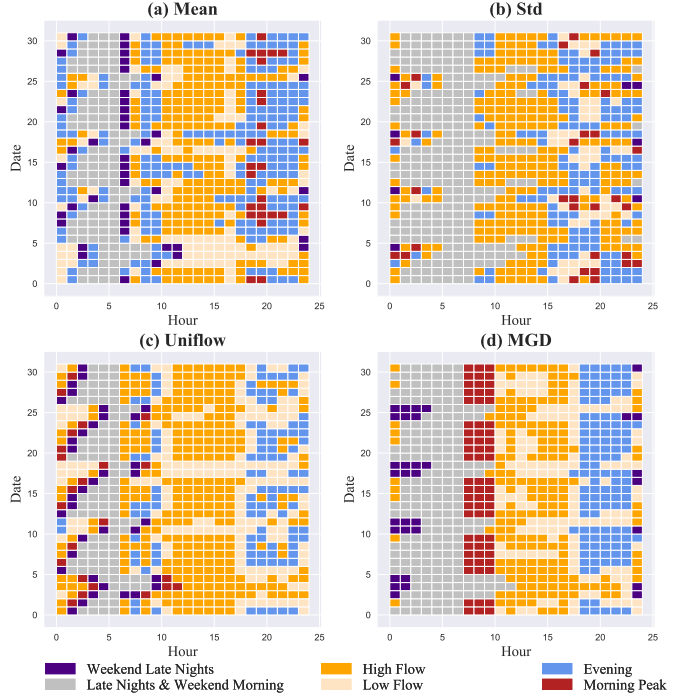


Figure 5: Comparison of clustering results using different distances. A certain color represents a specific pattern corresponding to the law of human mobility. MGD could distinguish important patterns (Figure 5.d), for example, morning peak (red), evening peak (blue), and weekend late night (purple).

named as MGFN-MGF, MGFN-IPMP and MGFN-IPMCA, respectively. Figure 4 shows the MAE, ARI and RMSE results of MGFN and its variants in crime prediction, land usage classification and check-in prediction tasks respectively. We observe that MGFN performs better than MGFN-MGF, demonstrating that the MGF module effectively eases the redundant temporal information for learning more general representations of urban regions. Moreover, MGFN consistently outperforms MGFN-IPMP and MGFN-IPMCA, which indicates the effectiveness of intra message passing and aggregating between nodes in each mobility pattern and inter messages fusion between mobility patterns in modeling the complex spatial correlations.

¹opendata.cityofnewyork.us

Table 1: Performance comparison with different methods for crime prediction, land usage classification and check-in count prediction tasks.

	Crime Prediction			Land Usage Classification		Check-in Prediction		
	MAE	RMSE	R ²	NMI	ARI	MAE	RMSE	R ²
LINE	117.53	152.43	0.06	0.17	0.01	564.59	853.82	0.08
node2vec	75.09	104.97	0.49	0.58	0.35	372.83	609.47	0.44
HDGE	72.65	96.36	0.58	0.59	0.29	399.28	536.27	0.57
ZE-Mob	101.98	132.16	0.20	0.61	0.39	360.71	592.92	0.47
MV-PN	92.30	123.96	0.30	0.38	0.16	476.14	784.25	0.08
MVURE	65.16	88.19	0.64	0.78	0.59	297.72	495.27	0.63
MG-FN	59.45	77.60	0.72	0.76	0.58	280.91	436.58	0.72

4.4 Graph Similarity Measurement (RQ3)

To intuitively evaluate the performance of the proposed Mobility Graph Fusion module (Section 3.1), we visualize the mobility patterns extracted by our multi-graph distance (MGD) measurement compared with three measures in Section 3.1 including Mean, Std, and Uniflow using hierarchical clustering. Specifically, in Figure 5, a certain color represents a specific pattern corresponding to the law of human mobility. We observe that different from other three measures, our MGD (Figure 5.d) is able to distinguish patterns of both morning/evening peaks and working days/weekends effectively, due to our integrated considerations with spatio-temporal information. We argue that this improvement is beneficial to enabling the cross-domain prediction (i.e., from traffic prediction to crime and check-in prediction) by uncovering the dynamic correlations contained in urban regional functionality.

4.5 Generalization Ability of MGFN (RQ4)

To show the generalization ability of our method, we compare the proposed MGFN with other three methods on both supervised task (i.e., mobility prediction) and cross-domain task (i.e., crime prediction) in Figure 6. Other methods perform poorly on cross-domain tasks because they learn how traffic changes rather than a generalized region representation. Moreover, after removed MGF, the generalization performance is reduced by about 20%, that shows the importance of MGF.

5 Related Works

Graph Representation Learning Graph embedding aims to learn a low-dimensional vector by mapping the characteristics of nodes to a low-dimensional vector space so that the proximities of nodes can be well preserved [Cui *et al.*, 2018]. Early works devote to learn the shallow representations by graph factorization approaches [Belkin and Niyogi, 2001] relying on spectral embedding from graph Laplacian and skip-gram based methods [Perozzi *et al.*, 2014; Grover and Leskovec, 2016; Tang *et al.*, 2015] learned by random walk objectives. More recently, graph neural networks (GNNs) have become a widely used tool for graph embedding [Veličković *et al.*, 2017; Gilmer *et al.*, 2017].

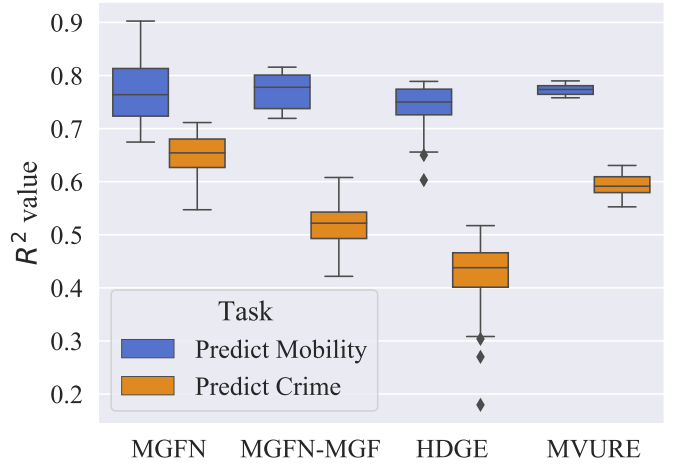


Figure 6: The generalization ability of our MGFN compared with three other methods. There are two observation: 1) All performance are similar in predicting mobility, and 2) MGFN outperforms other methods by over 10% for crime prediction.

Region Representation Learning Several strategies have been studied to learn the representation of regions. The first strategy learns embeddings from time-series human mobility data. HDGE [Wang and Li, 2017] uses fine-grained human mobility to construct flow graph, and learn the region embedding at different times. ZE-mob [Yao *et al.*, 2018] regards the region as a word and the mobility event as context, and learn the embedding via a word embedding method. The second strategy learns embeddings from multi-view cross-geotype(region and other spatio-temporal items) correlations. Fu *et al.* [2019] take into account both intra-region structural information and inter-region spatial auto-correlations. Zhang *et al.* [2020] use a cross-view information sharing method to learn comprehensive region embeddings.

6 Conclusion

In this paper, we focus on learning generalized embeddings to enable cross domain urban computing tasks. We proposed: (1) a novel mobility graph fusion method where redundant graphs are integrated as patterns; and (2) a novel mobility pat-

tern joint learning method to enable the cross graph embeddings that mutually enhance each other and provide more effective representation for downstream tasks. Extensive experiments on real-world mobility data show the proposed MGFN outperforms all baseline methods. Besides, in-depth analysis reveals insightful observations, e.g., Late nights and evenings on weekends show a different pattern from workdays. In future, we will extend our framework to other downstream tasks (e.g., house price prediction).

References

- [Belkin and Niyogi, 2001] Mikhail Belkin and Partha Niyogi. Laplacian eigenmaps and spectral techniques for embedding and clustering. In *Nips*, volume 14, pages 585–591, 2001.
- [Cui *et al.*, 2018] Peng Cui, Xiao Wang, Jian Pei, and Wenwu Zhu. A survey on network embedding. *IEEE Transactions on Knowledge and Data Engineering*, 31(5):833–852, 2018.
- [Du *et al.*, 2019] J. Du, Y. Zhang, P. Wang, J. Leopold, and Y. Fu. Beyond geo-first law: Learning spatial representations via integrated autocorrelations and complementarity. In *2019 IEEE International Conference on Data Mining (ICDM)*, pages 160–169, Los Alamitos, CA, USA, nov 2019. IEEE Computer Society.
- [Fu *et al.*, 2019] Yanjie Fu, Pengyang Wang, Jiadi Du, Le Wu, and Xiaolin Li. Efficient region embedding with multi-view spatial networks: A perspective of locality-constrained spatial autocorrelations. *33rd AAAI Conference on Artificial Intelligence, AAAI 2019, 31st Innovative Applications of Artificial Intelligence Conference, IAAI 2019 and the 9th AAAI Symposium on Educational Advances in Artificial Intelligence, EAAI 2019*, pages 906–913, 2019.
- [Gilmer *et al.*, 2017] Justin Gilmer, Samuel S Schoenholz, Patrick F Riley, Oriol Vinyals, and George E Dahl. Neural message passing for quantum chemistry. In *International conference on machine learning*, pages 1263–1272. PMLR, 2017.
- [Grover and Leskovec, 2016] Aditya Grover and Jure Leskovec. node2vec: Scalable feature learning for networks. In *Proceedings of the 22nd ACM SIGKDD international conference on Knowledge discovery and data mining*, pages 855–864, 2016.
- [He *et al.*, 2016] Kaiming He, Xiangyu Zhang, Shaoqing Ren, and Jian Sun. Deep residual learning for image recognition. In *Proceedings of the IEEE conference on computer vision and pattern recognition*, pages 770–778, 2016.
- [Hou and Li, 2016] Zhongsheng Hou and Xingyi Li. Repeatability and similarity of freeway traffic flow and long-term prediction under big data. *IEEE Transactions on Intelligent Transportation Systems*, 17(6):1786–1796, 2016.
- [Perozzi *et al.*, 2014] Bryan Perozzi, Rami Al-Rfou, and Steven Skiena. Deepwalk: Online learning of social representations. In *Proceedings of the 20th ACM SIGKDD international conference on Knowledge discovery and data mining*, pages 701–710, 2014.
- [Tang *et al.*, 2015] Jian Tang, Meng Qu, Mingzhe Wang, Ming Zhang, Jun Yan, and Qiaozhu Mei. Line: Large-scale information network embedding. In *Proceedings of the 24th International Conference on World Wide Web, WWW '15*, page 1067–1077, Republic and Canton of Geneva, CHE, 2015. International World Wide Web Conferences Steering Committee.
- [Tibshirani, 1996] Robert Tibshirani. Regression shrinkage and selection via the lasso. *Journal of the Royal Statistical Society: Series B (Methodological)*, 58(1):267–288, 1996.
- [Vaswani *et al.*, 2017] Ashish Vaswani, Noam Shazeer, Niki Parmar, Jakob Uszkoreit, Llion Jones, Aidan N Gomez, Łukasz Kaiser, and Illia Polosukhin. Attention is all you need. In *Advances in neural information processing systems*, pages 5998–6008, 2017.
- [Veličković *et al.*, 2017] Petar Veličković, Guillem Cucurull, Arantxa Casanova, Adriana Romero, Pietro Lio, and Yoshua Bengio. Graph attention networks. *arXiv preprint arXiv:1710.10903*, 2017.
- [Wang and Li, 2017] Hongjian Wang and Zhenhui Li. Region representation learning via mobility flow. *International Conference on Information and Knowledge Management, Proceedings*, Part F1318:237–246, 2017.
- [Wu *et al.*, 2021] Shangbin Wu, Xiaoliang Fan, Longbiao Chen, Ming Cheng, and Cheng Wang. Predicting the spread of covid-19 in china with human mobility data. In *Proceedings of the 29th International Conference on Advances in Geographic Information Systems, SIGSPATIAL '21*, page 240–243, New York, NY, USA, 2021. Association for Computing Machinery.
- [Xia *et al.*, 2021] Lianghao Xia, Chao Huang, Yong Xu, Peng Dai, Liefeng Bo, Xiyue Zhang, and Tianyi Chen. Spatial-temporal sequential hypergraph network for crime prediction with dynamic multiplex relation learning. In Zhi-Hua Zhou, editor, *Proceedings of the Thirtieth International Joint Conference on Artificial Intelligence, IJCAI-21*, pages 1631–1637. International Joint Conferences on Artificial Intelligence Organization, 8 2021. Main Track.
- [Xu *et al.*, 2020] Fengli Xu, Yong Li, and Shusheng Xu. Attentional Multi-Graph Convolutional Network for Regional Economy Prediction with Open Migration Data, page 2225–2233. Association for Computing Machinery, New York, NY, USA, 2020.
- [Yao *et al.*, 2018] Zijun Yao, Yanjie Fu, Bin Liu, Wangsu Hu, and Hui Xiong. Representing urban functions through zone embedding with human mobility patterns. *IJCAI International Joint Conference on Artificial Intelligence*, 2018-July:3919–3925, 2018.
- [Zhang *et al.*, 2020] Mingyang Zhang, Tong Li, Yong Li, and Pan Hui. Multi-view joint graph representation learning for urban region embedding. In Christian Bessiere, editor, *Proceedings of the Twenty-Ninth International Joint*

Conference on Artificial Intelligence, IJCAI-20, pages 4431–4437. International Joint Conferences on Artificial Intelligence Organization, 7 2020. Special track on AI for CompSust and Human well-being.